BIOCHEMISTRY
including biophysical chemistry & molecular biology
Article

Biochemistry **2011,** *50,* 1691–1699 1691
DOI: 10.1021/bi101654w

Novel Mechanism of the Vascular Protector Prostacyclin: Regulating MicroRNA Expression†

Anita Mohite, Annirudha Chillar, Shui-Ping So, Vanessa Cervantes, and Ke-He Ruan*

Center for Experimental Therapeutics and PharmacoInformatics and Department of Pharmacological and Pharmaceutical Sciences, College of Pharmacy, University of Houston, Houston, Texas 77004, United States

Received October 14, 2010; Revised Manuscript Received January 18, 2011

ABSTRACT: Prostacyclin (PGI_2) is a key vascular protector, metabolized from endogenous arachidonic acid (AA). Its actions are mediated through the PGI_2 receptor (IP) and nuclear receptor, peroxisome proliferator-activated receptor γ (PPARγ). Here, we found that PGI_2 is involved in regulating cellular microRNA (miRNA) expression through its receptors in a mouse adipose tissue-derived primary culture cell line expressing a novel hybrid enzyme gene (COX-1-10aa-PGIS), cyclooxygenase-1 (COX-1) and PGI_2 synthase (PGIS) linked with a 10-amino acid linker. The triple catalytic functions of the hybrid enzyme in these cells successfully redirected the endogenous AA metabolism toward a stable and dominant production of PGI_2. The miRNA microarray analysis of the cell line with upregulated PGI_2 revealed a significant upregulation (711, 148b, and 744) and downregulation of miRNAs of interest, which were reversed by antagonists of the IP and PPARγ receptors. Furthermore, we also found that the insulin-mediated lipid deposition was inhibited in the PGI_2-upregulated adipocytes. The study also initiated a discussion that suggested that the endogenous PGI_2 inhibition of lipid deposition in adipocytes could involve miRNA-mediated inhibition of expression of the targeted genes. This indicated that PGI_2−miRNA regulation could exist in broad pathophysiological processes involving PGI_2 (i.e., apoptosis, vascular inflammation, cancer, embryo implantation, and obesity).

Prostacyclin (PGI_2)[1] is the most potent endogenous vascular protector because it inhibits platelet aggregation and opposes the vasoconstricting and platelet pro-aggregating functions of thromboxane A_2 (TXA_2) (*1*, *2*). Thus, prostacyclin plays a key role in the prevention of atherosclerosis and other cardiovascular diseases (*3*). PGI_2 mediates its biological effects by binding to cell surface prostacyclin receptors (IPs), which couple to the stimulatory G protein (Gs) to activate adenylyl cyclase and increase the level of cyclic AMP (cAMP) (*4*, *5*). In addition to activating plasma membrane receptors, PGI_2 can also activate the nuclear receptors, peroxisome proliferator activated receptors (PPARs), which function as nuclear transcription factors. The PPAR family includes three isoforms, α, δ (β), and γ (*6*, *7*), which are activated by a broad spectrum of ligands. These include metabolites of the COX and lipoxygenase pathway and hypolipidemic agents, e.g., fibrates, which regulate inflammation, lipid metabolism, and insulin sensitivity (*8*, *9*). PPARγ, which is mostly expressed in the adipose tissue, large intestine, and spleen (*10*), is also the only PPAR that can be activated through the IP using stable PGI_2 analogues (*11*). Thus, prostacyclin can be directly related to lipid metabolism through the IP/PPARγ receptor. To date, there is conflicting evidence regarding a PGI_2-induced increase or decrease in the level of adipogenesis (*12*, *13*). However, logically, an early loss of endothelial PGI_2 could lead to deposition of the adipocyte lipid in the periphery and vascular smooth muscle cells (atherosclerosis). Currently, atherosclerosis is characterized by inflammation that causes vascular endothelial damage (*14*). The first step in the development of atherosclerosis is the formation of the fatty streak. The current accepted concept is that when LDL levels increase, they accumulate in the arterial intima and become oxidized into proinflammatory particles. This provokes an innate inflammatory reaction within the intima, and thus, fat droplets accumulate in the cytoplasm of smooth muscle cells. The resulting hemodynamic stress causes intimal thickening of the artery. When the monocytes enter the artery, they transform into macrophages, take up lipids, and become foam cells (*15*, *16*). However, we propose that the localized loss of the autocrine and paracrine effect of endothelial PGI_2 could be responsible for the subendothelial deposition of lipid in the smooth muscle cells of the vascular walls. It is known that lipid deposition in the vessel wall begins as fatty streaks at a very early age (*15*, *16*). This could represent an early loss of PGI_2 paracrine function.

We further propose that this lipid deposition can be confirmed by identification of appropriate specific proteins involved in the lipogenesis pathway. We have used primary culture recombinant DNA technology, mass spectrometric analysis, a microRNA (miRNA) microarray, and an RNA illumina assay to identify the pathway that links PGI_2 to lipid deposition. The source of PGI_2 was a hybrid enzyme that links COX-1 with PGIS through a designed linker. This hybrid enzyme was overexpressed in a primary culture of mouse adipocytes called "PGI_2-prostanoid-synthesizing fat cells" (PGI_2-PSFCs) (*17*−*19*). The hybrid enzyme was able to integrate the triple catalytic functions of COX and PGIS into one enzyme (named Tri-Cat enzyme) and effectively and

†This work was supported by the National Institutes of Health (Grants HL56712 and HL79389 to K.-H.R.) and the American Heart Association (Grant 10GRNT4470042 to K.-H.R.).

*To whom correspondence should be addressed: University of Houston, 4800 Calhoun Rd., SR2, Rm. 521, Houston, TX 77004-5037. Fax: (713) 743-1884. Telephone: (713) 743-1771. E-mail: khruan@uh.edu.

[1]Abbreviations: PGI_2, prostacyclin; AA, arachidonic acid; miRNA, microRNA; PGI_2-PSFCs, PGI_2-prostanoid-synthesizing fat cells.

Published on Web 01/20/2011

continuously convert endogenous arachidonic acid (AA) into PGI_2 (*17*−*19*).

We evaluated the regulation of miRNAs in adipocytes and PGI_2-PSFCs because they makw up a novel class of endogenous, small, noncoding RNAs that base pair with their target mRNAs leading to mRNA degradation or repression of translation (*20*, *21*). Thus, they are endogenous, negative regulators of gene expression that are involved in the regulation of cell proliferation and growth, mobility, differentiation, and apoptosis (*22*−*26*). Consequently, deregulated miRNA function may result in diseases of the heart (*27*) and liver, immune dysfunction, cancer (*24*, *28*), and metabolic disorders (*29*−*31*). This was the first verification that endogenous PGI_2 could inhibit lipid deposition in adipocytes possibly with the involvement of regulation of miRNA expression.

The cell-based method used to study the autocrine and paracrine effect of PGI_2 in the primary culture of adipocytes is novel in that it allows us to study endogenous PGI_2 that has a very short half-life. This method allows us to closely mimic the in vivo effect of PGI_2 produced by endothelial cells and predict the pathway involved in lipid deposition.

EXPERIMENTAL PROCEDURES

Materials. Media, such as Dulbecco's modified Eagle's medium type F-12 (DMEM-F12), newborn calf serum (NCS), antibiotic and antimycotic, Geneticin (G418), and TRIZOL for culturing the cell lines were purchased from Invitrogen (Carlsbad, CA). The following were purchased from Cayman Chemical Co. (Ann Arbor, MI): CAY 10441 (IP antagonist), GW9662 (PPARγ antagonist), and primary antibodies against human COX-1 and PGIS. The miRNA isolation kit, RT^2 miRNA First Strand Kit, RT^2 SYBR Green qPCR Master Mix, the primer for miRNA 711, and sno RNA 142 were purchased from SA Biosciences (Frederick, MD). The primary antibody against Akt1 was purchased from Santa Cruz Biotechnology (Santa Cruz, CA). Oil Red O was purchased from Sigma Aldrich (St. Louis, MO).

Engineered cDNA Plasmids with Single Genes Encoding the Human COX-1 and PGIS Sequences. The sequence of COX-1 linked to PGIS through a 10-amino acid (10aa) linker (COX-1-10aa-PGIS, Trip-cat enzyme-1) was generated by a PCR approach and subcloning procedures previously described (*18*).

Establishing a Primary Cultured Cell Line Derived from Adipose Tissue. Inguinal adipose tissue, excised from a C57BL/6 mouse, was washed thoroughly with phosphate-buffered saline (pH 7.5) and then digested with collagenase (2 mg/mL) at 37 °C for 1 h. The digested adipose tissue was then filtered through glass wool and subjected to low-speed centrifugation for further separation. The mature adipocytes collected from the upper layer of the collagenase-digested mouse adipose tissue were placed between two cover slides in a 10 cm cell culture dish with DMEM-F12 containing 10% newborn calf serum (NCS) and 1% antibiotic and antimycotic and then were grown at 37 °C in a humidified 5% CO_2 incubator. After 15 days, the lipid droplets within the cells completely disappeared. Furthermore, the cells had converted into attached "fat cells" with the capacity to synthesize endogenous prostanoids and were termed prostanoid-synthesizing fat cells (PSFCs). The protocol was approved by the Animal Safety Committee of the University of Houston.

Stable Expression of the Trip-cat Enzyme-1 in the Cultured Fat Cells. The PSFCs were grown and transfected with purified pcDNA3.1-COX-1-10aa-PGIS by the Lipofectamine 2000 method following the manufacturer's instructions (Invitrogen). For stable expression, the transfected cells were cultured in the presence of G418 screening for several weeks following the manufacturer's instructions. The cells stably expressing Trip-cat enzyme-1 were identified by Western blot analysis and liquid chromatography−mass spectrometry (LC−MS) analysis.

Determination of the Endogenous AA Metabolism in Fat Cells Using LC−*MS*. Simultaneous quantification of AA metabolites in the cultured PSFCs (with and without transfection of the Trip-cat enzyme-1 cDNA) was detected by LC−MS following the reported methods (*17*, *18*). Briefly, the cell culture medium was collected and applied to a C18 cartridge (Honeywell Burdick & Jackson, model BJ9575). After being washed with water, the AA metabolites bound to the cartridge were eluted with acetone, dried with nitrogen gas, and then dissolved in solvent A (0.1% acetic acid and 35% acetonitrile). The sample was injected into the Waters Micromass LC−MS/MS system with an autosampler. The metabolites are first separated by the RP-HPLC C18 column and then automatically injected into the mass detector equipped with an ESI source in a negative mode. Synthetic AA and 6-keto-$PGF_{1\alpha}$, obtained from Cayman Chemical Co., were used as standards to calibrate the LC−MS system, identify the corresponding prostanoids, and normalize the detection limits and sensitivities.

Immunoblot Analysis. The stable transfected cells (PGI_2-PSFCs) expressing Trip-cat enzyme-1 or those PSFCs transfected with vector (pcDNA 3.1) alone were collected and washed with PBS. Membrane proteins were separated by 10% (w/v) sodium dodecyl sulfate−polyacrylamide gel electrophoresis under denaturing conditions and then transferred to a nitrocellulose membrane. Bands recognized by specific primary antibodies (PGIS, COX-1, or cPGES) were visualized with horseradish peroxidase-conjugated secondary antibody.

MiRNA Microarray Analysis. PSFCs and PGI_2-PSFCs were cultured as described above, and after 24 h, the total RNA was isolated using TRIZOL. In another experiment, PGI_2 adipocytes were serum starved for 5−6 h, and then one plate was treated with IP antagonist CAY10441 (1 μM) and the other with PPARγ antagonist GW9662 (5 μM). After 24 h, total RNA was isolated. Total RNA samples were analyzed by LC Sciences (Houston, TX), which provided microarray analyses. Once their results have been collected, a search was performed on the target genes of the individual miRNAs using the website http://microrna.sanger.ac.uk.

Quantitative Real-Time PCR (*qRT-PCR*). The level of miRNA 711 was measured by the qRT-PCR approach using three kits obtained from SA Biosciences following the detailed instructions in the kits. First, the miRNAs were isolated from the cultured PGI_2-PSFCs or control PSFCs using the RT^2 qPCR-Grade miRNA Isolation Kit. Second, the isolated miRNAs were converted into cDNAs using the RT^2 miRNA First Strand Kit, and finally, the cDNAs were mixed with another kit, RT^2 SYBR Green qPCR Master Mix, the primer for miRNA 711, and sno RNA 142 (control) and then analyzed by qPCR using the Applied Biosystems 7300 Real Time PCR System. Differential expression of miRNA 711 in the cells was analyzed by the $\Delta\Delta$CT method using mouse housekeeping sno RNA 142 (small nucleolar RNA) as a control. The levels of miRNA 711 in the cells were calculated using the formula $2^{(-\Delta\Delta Ct)}$ ($n = 5$).

Illumina Gene Expression Assay. Two hundred nanograms of total RNA from PSFCs and PGI_2-PSFCs was amplified and purified using the Illumina TotalPrep RNA Amplification Kit (Ambion, Inc.) following the manufacturer's instructions. Briefly, the first-strand cDNA was synthesized by incubating RNA with

T7 oligo(dT) primer and reverse transcriptase mix at 42 °C for 2 h. RNase H and DNA polymerase master mix were immediately added to the reaction mix following reverse transcription and were incubated for 2 h at 16 °C to synthesize second-strand cDNA. RNA, primers, enzymes, and salts that would inhibit in vitro transcription were removed through cDNA filter cartridges (part of the amplification kit). In vitro transcription was performed, and biotinylated cRNA was synthesized by a 14 h amplification with dNTP mix containing biotin-dUTP and T7 RNA polymerase. Amplified cRNA was subsequently purified, and the concentration was measured with a NanoDrop ND-1000 spectrophotometer (NanoDrop Technologies). An aliquot of 1.5 μg of amplified products was loaded onto Illumina Sentrix Beadchip Array Mouse-6 arrays, hybridized at 58 °C in an Illumina Hybridization Oven (Illumina, Inc.) for 17 h, washed, and incubated with streptavidin-Cy3 to detect biotin-labeled cRNA on the arrays. Arrays were dried and scanned with a BeadArray Reader (Illumina, Inc.). Data were analyzed using BeadStudio (Illumina, Inc.). Clustering and pathway analysis were performed with BeadStudio and Ingenuity Pathway Analysis (Ingenuity Systems, Inc.), respectively.

Akt1 Immunoblot. Cells were harvested and lysed in lysis buffer [50 mM Tris-HCl (pH 7.4), 1% Triton X-100, 150 mM NaCl, 1 mM EDTA, 1 mM phenylmethanesulfonyl fluoride, 1% aprotinin, 10 mg/mL leupeptin, 1 mM sodium orthovanadate, and 1 mM sodium fluoride]. Cell lysates were centrifuged at 12000*g* for 10 min at 4 °C. The protein concentration of the cell lysate was determined by performing the BCA protein assay. Sodium dodecyl sulfate−polyacrylamide gel electrophoresis sample buffer was added to the lysates, which were then heated to 100 °C for 5 min; 25 μg of protein was loaded in each well of the 10% acrylamide gel and separated by electrophoresis. Proteins were transferred onto a nitrocellulose membrane, which was incubated with primary antibody against Akt1 and a horseradish peroxidase-conjugated secondary antibody. Chemiluminescence was detected using an ECL Kit (Amersham).

Lipid Accumulation in PSFCs and PGI_2-PSFCs. PSFCs and PGI_2-PSFCs were grown to 50% confluency in DMEM-F12 medium containing 10% newborn calf serum. This medium was then replaced with adipogenic medium [DMEM containing 10% fetal bovine serum (FBS), 1 μM dexamethasone (Sigma-Aldrich), 0.5 mM isobutylmethylxanthine (IBMX), and insulin (10 μg/mL)], and the cells were allowed to grow in this medium for 4 days. After 4 days, the cells were refed with DMEM-F12 medium containing 10% FBS and 10 μg/mL insulin and were grown for an additional 3 days. Images were taken every day to observe cells that were accumulating lipid droplets.

Oil Red O Staining. After the cells had been treated with differentiation medium for 7 days, the accumulation of intracellular lipid was assessed via Oil Red O (Sigma-Aldrich) staining. A 0.36% (w/v) solution of Oil Red O was prepared in 60% 2-propanol. The cells were washed twice with PBS and fixed with 4% paraformaldehyde for 5 min and then washed with PBS and 2-propanol. The cells were then stained with an Oil Red O solution for 30 min and rinsed with 2-propanol. Cells were observed via a light microscope with 100× magnification and then photographed using a Kodak DC 290 Zoom Digital Camera.

RESULTS

Isolation, Culture, and Conversion of the Mature Adipocytes into Attached Prostanoid-Synthesizing Fat Cells (PSFCs). In this study, the isolated mouse mature adipocytes (Figure 1a, day 1) were placed between cover slides and cultured in DMEM-F12 medium for 10 days in 10 cm cell culture dishes; the cells became attached to the slides, and lipid droplets completely disappeared (Figure 1a, day 10). The attached cells were termed prostanoid-synthesizing fat cells (PSFCs) because the cells could metabolize endogenous AA into prostanoids. Figure 1d (panel i, top graph) shows the profile of the AA standard [molecular weight (MW) of 305] as presented by LC−MS analysis with an ESI source in a negative mode. On the other hand, the LC−MS analysis of the PSFCs shown in the bottom graph (Figure 1d, panel i) demonstrates the conversion of endogenous AA into primarily PGE_2 (MW of 351) as evidenced by LC−MS analysis with an ESI source in a negative mode.

Redirecting the PSFC Line To Specifically Convert Endogenous AA into PGI_2, Thereby Forming the PGI_2-PSFC Line. In our previous studies, we have shown that by overexpressing our novel Trip-cat enzyme-1 (COX-1-10aa-PGIS, human COX-1 linked to PGIS) in HEK293 cells, we were able to direct the conversion of endogenous AA into a stable overproduction of PGI_2 (*18*). Similarly, the endogenous AA that was metabolized into PGE_2 [by the endogenous cPGES (Figure 1b)] in the PSFC line was redirected to produce PGI_2 in the PSFC line overexpressing Trip-cat enzyme-1 (PGI_2-PSFC line). This stable overexpression of COX-1-10aa-PGIS was identified by Western blot analysis (Figure 1c). The resultant endogenous metabolism of AA into PGI_2 was confirmed by LC−MS analysis (Figure 1d, panel ii). Here, the top graph shows the analysis of the 6-keto-$PGF_{1\alpha}$ (PGI_2 stable byproduct) standard, and the bottom graph represents that of the PGI_2-PSFCs, which effectively converted the endogenous AA into primarily PGI_2 (shown as 6-keto-$PGF_{1\alpha}$). Thus, this cell line was termed the PGI_2-PSFC line, an exceptional model for studying the biological functions of continuously produced, unstable PGI_2 from the endogenous AA.

Detection of MiRNA Expression in PGI_2-PSFCs. The miRNA microarray analysis of the total RNA in the cultured PGI_2-PSFCs (Figure 2a, panel ii) showed a significant change in the expression levels of 114 miRNAs in the cells. The expression levels of these miRNAs in the nontransfected PSFCs (derived from the same source of adipocytes) were used as a control (Figure 2a, panel i). High-quality signals for the miRNAs in both cells were obtained. From these analyses, we determined that after comparison with the control (Figure 2a, panel i), several miRNAs in the PGI_2-PSFCs (Figure 2a, panel ii) were either upregulated (circles) or downregulated (squares).

Profile of the MiRNAs That Are Upregulated by the Endogenous PGI_2 in PGI_2-PSFCs. After comparing the expression levels of miRNAs in the PGI_2-PSFCs and the PSFC control cells, we observed that 64 of 114 miRNAs exhibited different degrees of increase. Of these 64 miRNAs, five exhibited an increase of more than 2-fold (Figure 2b). There were approximate 15-, 4-, and 3-fold increases in miRNAs 711, 31*, and 720, respectively (Figure 2b). Interestingly, these miRNAs have predicted target genes (http://microrna.sanger.ac.uk) that are associated with adipocyte differentiation, atherosclerosis, tumors, and brain angiogenesis as listed in Table 1. Therefore, we postulate that upregulated miRNAs in PGI_2-PSFCs will inhibit the expression of these target genes and thus have a protective role in atherosclerosis and tumors. In particular, the expression level of the miRNA 711 increased by almost 15-fold (Figure 2b), making this a very significant observation because endogenous PGI_2 could be a powerful upregulator for miRNA 711 expression in mammalian cells.

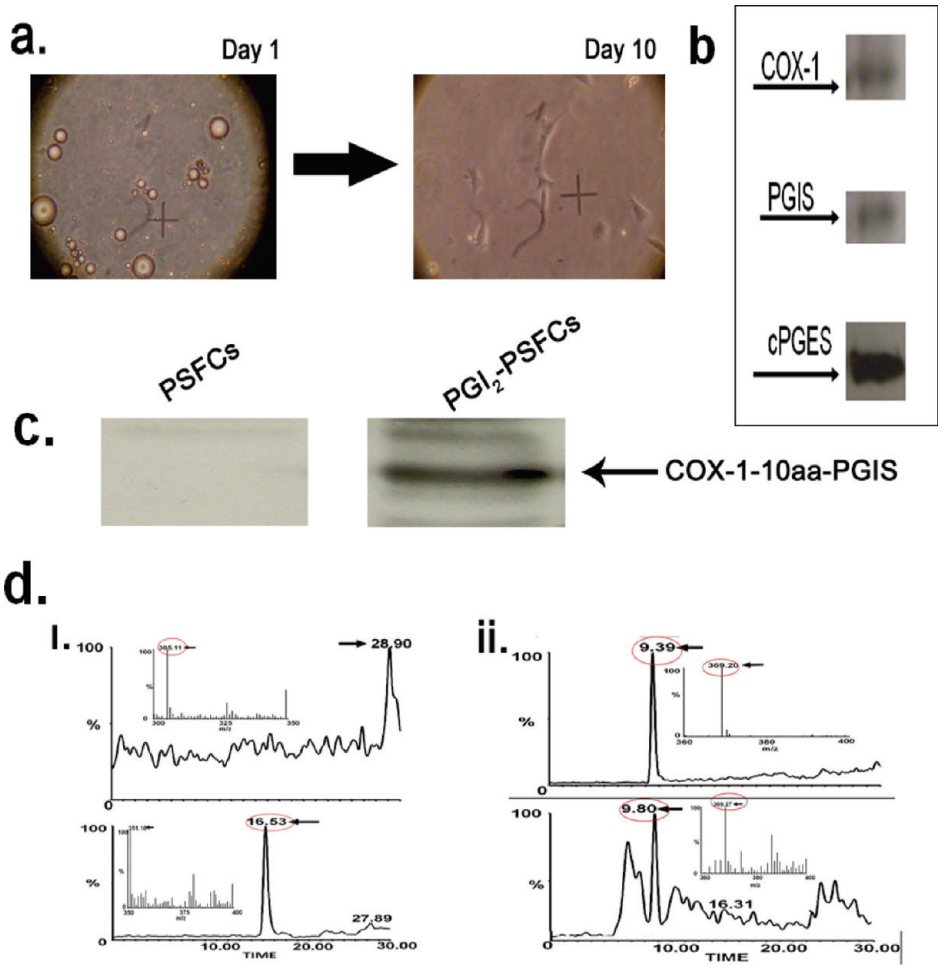

FIGURE 1: (a) Conversion of mouse mature adipocytes (day 1) into attached PSFCs (day 10). (b) Western blot showing endogenous COX-1, PGIS, and cPGES in the control PSFCs. (c) Western blot showing PSFCs (lane 1) and the stable expression of COX-1-10aa-PGIS transfected in PSFCs to generate PGI_2-PSFCs (lane 2). (d) LC−MS analysis of PSFCs (panel i, bottom graph) and PGI_2-PSFCS (panel ii, bottom graph). The top graphs in panels i and ii show data for the standard AA (retention time of 28.9 min with a molecular weight of 305) and 6-keto-$PGF_{1\alpha}$ (retention time of 9.8 min with a molecular weight of 369), respectively.

Profile of the MiRNAs That Are Downregulated by the Endogenous PGI_2 in PGI_2-PSFCs. There were 54 miRNAs downregulated by PGI_2 in the PGI_2-PSFCs when compared with the control PSFCs. The top five miRNAs with a more than 5-fold decrease in their expression levels are shown in Figure 2b, and the target genes for these miRNAs are listed in Table 2. The most significantly downregulated miRNA is the 466f-3p (13.5-fold decrease), which might regulate the expression of target genes whose biological function is associated with lipid clearance, tumors, and apoptosis (Table 2). There was also an approximate 10-fold decrease in the levels of miRNAs 148a and 467b*, which have functions similar to that of 466f-3p. It was also worth noting that a 4-fold decrease in the levels of miRNAs 206 and 574-5p (data not shown), whose predicted target genes are embryonic ectoderm development, could suggest that PGI_2 plays a role in embryonic development.

Inhibition of Upregulated MiRNA Expression in PGI_2-PSFCs Using the PPARγ Antagonist. PGI_2-PSFCs were treated with the PPARγ antagonist GW 9662 (5 μM) for 24 h, and the total RNA was isolated and analyzed with a microarray (Figure 3a, panel i). Interestingly, the effects of the endogenous PGI_2-upregulated and -downregulated miRNAs' expression in the PGI_2-PSFCs were inhibited (Figure 3b, panel i). It was particularly interesting to note that levels of miRNAs 711 and 466f-3p, whose expression levels were up- and downregulated more than 12-fold by PGI_2 signaling (Figure 2b), returned to their basal level or below it (Figure 3b, panel i). This result indicated that (1) PPARγ signaling is involved in regulating miRNA expression in mammalian cells, (2) PGI_2-mediated upregulation and downregulation of miRNA expression could occur through PPARγ, and (3) at least miRNA 711 and 466f-3p are targets for the endogenous PGI_2 signaling through PPARγ.

Inhibition of Upregulated MiRNA Expression in PGI_2-PSFCs Using the IP Antagonist. The effects of the IP antagonist (CAY 10441) on the changes in the expression of miRNAs in PGI_2-PSFCs were compared with that of the control PSFCs (Figure 3a, panel ii). Interestingly, the top five upregulated and downregulated miRNAs in the PGI_2-PSFCs were inhibited (Figure 3b, panel ii) like the PPARγ antagonist (Figure 3b, panel i). Again, the expression of the dramatically upregulated miRNA 711 and downregulated miRNA 466f-3p (by the PGI_2 signaling) was blocked by the IP antagonist (Figure 3b, panel ii). These results demonstrated that (1) upregulated and downregulated expression of miRNAs in PGI_2 cells indeed results from the PGI_2 produced by the cells, (2) both IP and PPARγ are involved in PGI_2 signaling, affecting miRNA expression, (3) there is likely a signaling molecule linking IP with PPARγ during the PGI_2 signaling, affecting miRNA expression, and (4) because the nuclear receptor, PPARγ, is directly involved in the regulation of gene expression, it can be deduced that

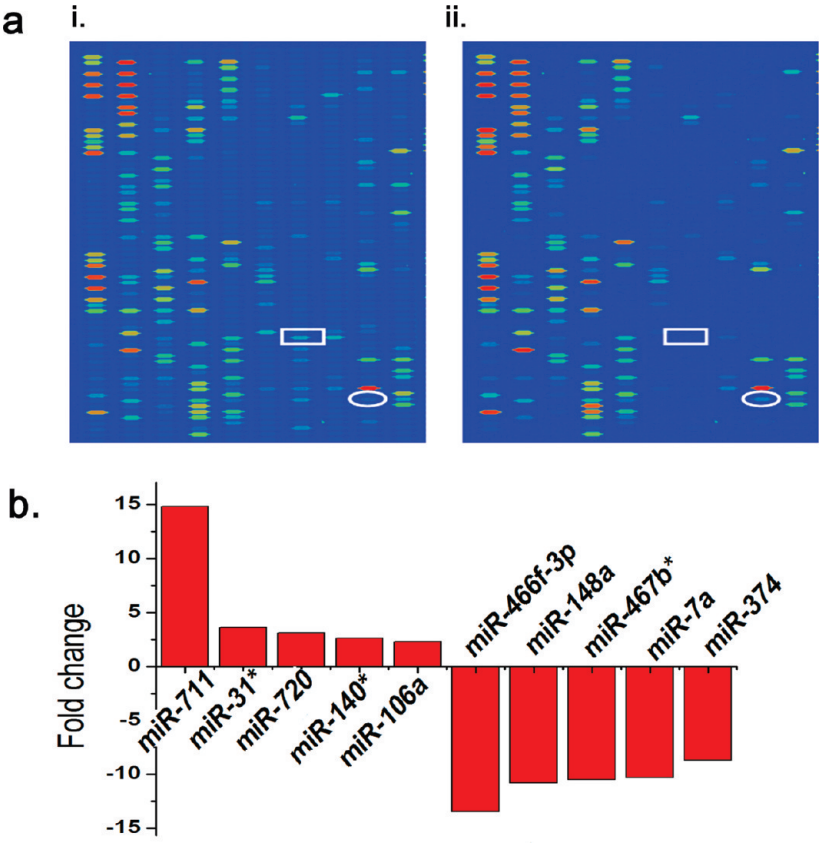

FIGURE 2: (a) MiRNA microarray profiles showing PSFC miRNA expression (panel i) and PGI_2-PSFC miRNA expression (panel ii). Ovals denote the expression profiles of the upregulated miRNA 711, and rectangles denote the expression profiles of the downregulated miRNA 466f-3p. (b) Increases and decreases in the top five miRNAs in PGI_2-PSFCs when compared to PSFCs.

Table 1: Upregulated miRNAs in the PGI_2-PSFCs and Their Predicted Target Genes and Biological Functions [Sanger MicroCosm Target - miRBase (http://microrna.sanger.ac.uk/targets/v5)]

upregulated miRNAs	predicted target genes	predicted biological function
miR-711	CCAAT/C/EBP β	↓ adipocyte differentiation
		↓ tumorigenesis
	CD160	↓ pathologic neovascularization
	Akt1	↓ adipogenesis, VSMC differentiation/proliferation, proliferation/invasion of malignant tumors, and vascular dysfunction in obesity
	lipase	↓ atherogenesis
miR-31*	PPARα	↓ adipocyte differentiation
	brain specific angiogenesis inhibitor	↓ angiogenesis
miR-720	lipase endothelial	↓ atherogenesis
miR-140*	amyloid β (A4) precursor protein-binding, family A	↓ Alzheimer's disease
	3-hydroxy-3-methylglutaryl-coenzyme A synthase 2	↓ ketogenesis
miR-106a	tumor susceptibility gene	↓ tumors

PPARγ is a downstream target and IP is an upstream target mediating the PGI_2 signaling for miRNA expression.

Quantitative Determination of MiRNA 711 Upregulated in PGI_2-PSFCs by the qRT-PCR Approach. We further validated the observation of the miRNAs regulated by PGI_2 in the PGI_2-PSFCs. The miRNA 711 that has the highest level upregulated in the cells was selected as a target for qRT-PCR analysis. As a result, the level of miRNA 711 in PGI_2-PSFCs was up to 6-fold higher than that of the control PSFCs (Figure 3c). This information is similar to that of the results of miRNA microarrays shown in panels a and b of Figure 2, in which the level of miRNA 711 expression was increased >10-fold, compared to that of the control cells. These quantitative data have further confirmed that miRNA 711 could be used as one of the miRNA targets to reveal the relationship between PGI_2 and miRNAs.

Inhibition of Accumulation of Lipid in PGI_2-PSFCs. There was a reduced level of accumulation of lipid droplets in PGI_2-PSFCs as compared to that in the control PSFCs detected by Oil Red O staining after 7 days (Figure 4). PGI_2-PSFCs did not accumulate lipid droplets when treated with adipogenic medium containing dexamethasone, IBMX, and insulin. This indicates that PGI_2, through the upregulation of miRNAs 711, 744, and 148b, could inhibit lipid accumulation (Figure 4).

Detection of Downregulated Akt1 MiRNA Using the Illumina Gene Expression Assay. This assay showed a >2-fold increase in the levels of 354 mRNAs and a >2-fold decrease in

Table 2: Downregulated miRNAs in the PGI_2-PSFCs and Their Predicted Target Genes and Biological Functions [Sanger MicroCosm Target - miRBase (http://microrna.sanger.ac.uk/targets/v5)]

downregulated miRNAs	predicted target genes	predicted biological function
miR-466f-3p	ABC1	↑ lipid clearance
	large tumor suppressor	↓ tumors
	lipase	↓ atherogenesis
miR-148a	ABC7	↑ lipid clearance
miR-467b*	CASP8 and FADD-like apoptosis regulator	↑ apoptosis regulation
miR-7a	insulin-induced gene 2, insulin receptor substrate 1 and 2	↑ insulin sensitivity
	block of proliferation 1	↓ proliferation
miR-374	suppression of tumorigenicity gene	↓ tumors

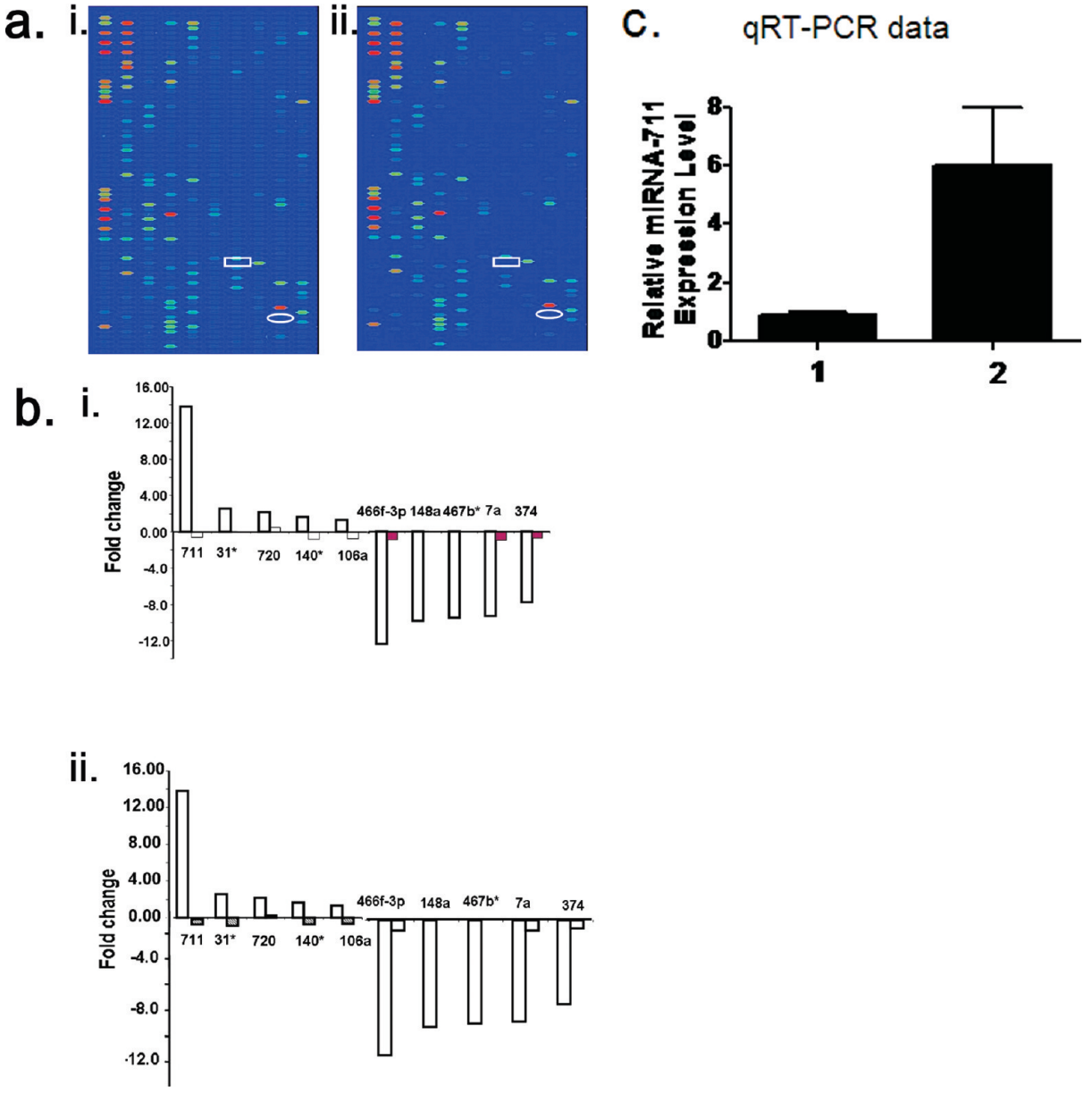

FIGURE 3: (a) MiRNA microarray profiles showing PGI_2-PSFC miRNA expression upon treatment with IP antagonist (panel i) and PPARγ antagonist (panel ii). Ovals denote the expression profiles of miRNA 711, and rectangles denote the expression profiles of miRNA 466f-3p. (b) Return to baseline of the upregulated and downregulated miRNA with PPARγ antagonist (panel i) or IP antagonist (panel ii) in PGI_2-PSFCs. (c) Comparison of the miRNA expression levels between the control PSFCs (1) and PGI_2-PSFCs (2). The level of miRNA 711 was measured by the qRT-PCR approach using RT^2 SYBR Green qPCR Master Mix, the primer for miRNA 711, and sno RNA 142 (housekeeping endogenous control) and then analyzed by qPCR using the Applied Biosystems 7300 Real Time PCR System. Differential expression of miRNA 711 in the cells was analyzed by the ΔΔCT method. The levels of miRNA 711 in the cells were calculated using the formula $2^{(-\Delta\Delta Ct)}$ ($n = 5$).

the levels of 471 mRNAs in PGI_2-PSFCs in comparison to PSFCs (data not shown). In addition, miRNA Akt1 was identified as being downregulated by 4-fold. Upregulated miRNAs 711 (Table 1), 744, and 148b, identified by microarray analysis, also have Akt1 as one of their gene targets [Sanger MicroCosm Target - miRBase (http://microrna.sanger.ac.uk/targets/v5)]. Upon

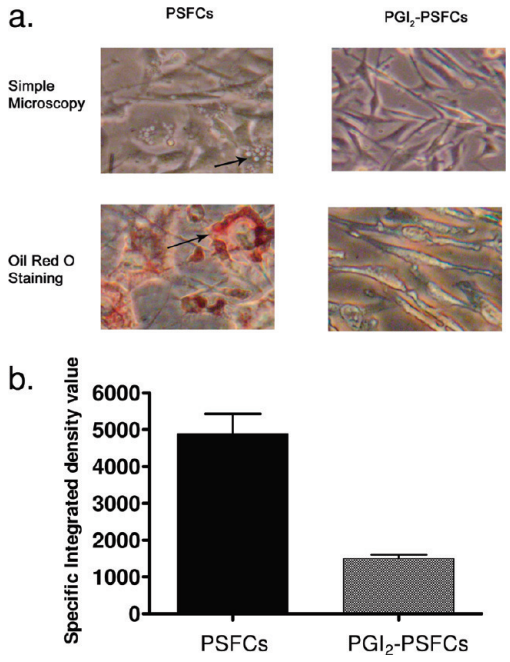

FIGURE 4: (a) Simple microscopy (row 1) of the PSFCs (the arrow indicates lipid droplets) and PGI_2-PSFCs. Oil Red O staining (row 2) of PSFCs (the arrow indicates the red color of lipid droplets) and PGI_2-PSFCs showing lipid accumulation. (b) Comparison of integrated density values between PSFCs and PGI_2-PSFCs. Intensities were determined using AlphaEase FC from Cell Biosciences (Santa Clara, CA) and taking values of five images.

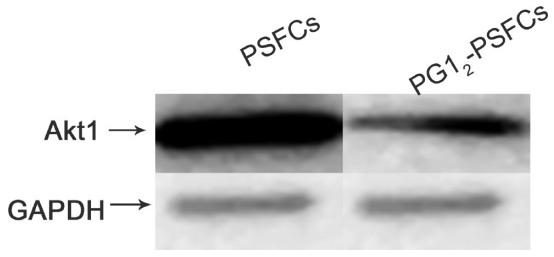

FIGURE 5: Western blots showing the expression of Akt1 in PSFCs (lane 1) and PGI_2-PSFCs (lane 2). GAPDH was used to normalize the expression level of Akt1.

comparison, it can be deduced that these miRNAs were possibly downregulating the level of Akt1 gene expression.

Downregulation of the Level of Akt1 Expression in PGI_2-PSFCs Using Immunoblot Analysis. Using a monoclonal Akt1 primary antibody, we detected the downregulation of the level of Akt1 expression in PGI_2-PSFCs (Figure 5, lane 2) as compared to PSFCs (Figure 5, lane 1). The experiment was normalized using the GAPDH primary antibody. This finding suggested that the upregulated miRNAs 711, 744, 148b may be downregulating the level of Akt1 gene expression.

DISCUSSION

The recombinant hybrid enzyme (COX-1-10aa-PGIS) overexpressed in a primary culture of mouse adipose tissue was able to integrate its triple catalytic functions of COX-1 and PGIS to effectively and continuously convert endogenous AA into PGI_2 (*17*−*19*). We were able to detect the stable production of PGI_2 through the presence of 6-keto-$PGF_{1\alpha}$ (the stable byproduct) using LC−MS (Figure 1d, panel ii). The miRNA microarray analysis of the PGI_2-PSFCs (expressing COX-1-10aa-PGIS) versus the vector-transfected primary culture adipocytes (PSFCs) showed that overproduction of PGI_2 causes an upregulation in miRNAs 711, 148b, and 744 and a downregulation in miRNAs 466f-3p, 148a, 7a, 374, etc. This PGI_2-induced miRNA regulation was IP- and PPARγ receptor-mediated because the effect was reversed by using CAY10441 (IP antagonist) and GW9662 (PPARγ antagonist) (Figure 3). Our experimental data showing the analyzed correlation between miRNA expression and IP/PPARγ blockade (Figure 3) have provided evidence that the effects of the miRNA expression were possibly related to the PGI_2 receptor mediation, as there was no difference between the IP and PPAR receptors. This raises the possibility that the two receptors may coordinate together for miRNA expression. Upregulation of miRNA 711 was further confirmed by quantification using quantitative real-time PCR.

MiRNAs regulate gene expression either by inhibiting mRNA translation or by causing degradation of mRNAs (*20*, *21*). MiRNA have been reported to play a role in adipogenesis of preadipocytes (*32*). By referring to a list of targets (http://microrna.sanger.ac.uk), we identified that C/EBP β is one of the predicted gene targets of miRNA 711 and the Akt1 gene is the predicted target of miRNA 711 (Table 1), 148b, and 744. Transcription factor C/EBP β/δ is known to mediate the transcriptional activation of PPARγ and C/EBP α, which in turn causes differentiation of adipocytes and induces maturation of preadipocytes into lipid-containing fat cells (*33*). Similarly, the phosphatidylinositol 3-kinase (PI3K)/Akt1 pathway regulates the process of adipocyte differentiation. It has been reported that the absence of Akt1/PKB α in primary mouse fibroblasts cells does not promote adipocyte differentiation (*34*). Akt1 in association with ProF has been suggested to produce phosphorylation of FoxO1 and thereby cause its nuclear export. This, in turn, results in the inactivation of FoxO1, which is a repressor of adipogenesis and a negative regulator of insulin actions (*35*, *36*). It is also reported that PGI_2, through its paracrine effect of inhibiting the Akt1 pathway, induces inhibition of vascular smooth muscle cell proliferation and prevents dedifferentiation, thus indicating its role as atheroprotective (*37*). This is a very complex system that has not yet been settled. Thus, we have initiated a very preliminary study for the regulation of gene expression through miRNA and performed an RNA illumina assay. The results showed many of the mRNA were upregulated and downregulated in the PGI_2-PSFCS when compared to the vector-transfected PSFCs (data not shown). From the assay, we were able to show that there was a downregulation of the level of mRNA Akt1 in PGI_2 adipocyte cells in comparison to the control adipocytes. Therefore, Akt1 may be a gene target of miRNA 711, 148b, and 744. We also observed the RNA illumina assay's downregulation of the level of mRNA Akt1 by performing an immunoblot assay of total Akt1 in both primary culture cell lines (Figure 5). However, confirmation of the relationship between Akt1 and PGI_2 requires many more intensive studies. Such studies would exceed our current experimental designs; however, they could be included in our future work.

Thus, identification of the signaling molecule, microRNA 711, indicated that PGI_2 plays a role in inhibiting lipid deposition and facilitating clearance (Tables 1 and 2). We further incubated our PGI_2-PSFCs and PSFCs (control) in adipogenic medium with insulin and found that there was a decreased level of lipid deposition in PGI_2-PSFCs when compared with control PSFCs (Figure 4). This shows that PGI_2 reduced the sensitivity of insulin-mediated lipid deposition in cells.

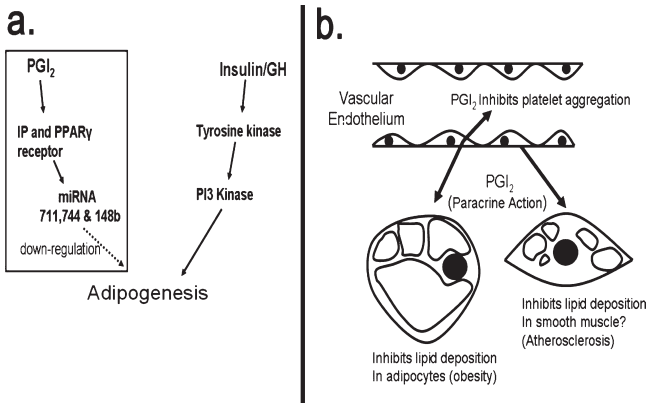

FIGURE 6: (a) Schematic showing the proposed mechanism of inhibition of adipogenesis by PGI_2. The box indicates the proposed pathway. (b) Proposed paracrine action as an application in obesity and atherosclerosis through upregulation of PGI_2 biosynthesis.

Our findings also predict that the loss of the paracrine and autocrine effect of endothelial PGI_2 could be responsible for early atherosclerosis as fatty streaks. These fatty streaks are lipid deposits in the smooth muscle cells underlying the PGI_2-producing endothelium (Figure 6). Our future efforts will be directed toward studying deposition of lipid in smooth muscle cell lines transfected with our PGI_2-producing hybrid enzyme.

In conclusion, our array data suggest that PGI_2 regulates miRNA expression that inhibits insulin-mediated lipid deposition in cells (Figure 6a). This is relevant because peripheral lipid deposition (obesity) and atherosclerosis, which is uncontrolled subendothelial lipid deposition in smooth muscle cells, could be directly related to impaired PGI_2 production as hypothesized (Figure 6b).

ACKNOWLEDGMENT

We thank Dr. Xiaolian Gao for her assistance with the miRNA-related studies.

REFERENCES

1. Moncada, S., Herman, A. G., Higgs, E. A., and Vane, J. R. (1997) Differential formation of prostacyclin (PGX or PGI_2) by layers of the arterial wall. An explanation for the anti-thrombotic properties of vascular endothelium. *Thromb. Res. 11*, 323–344.
2. Majerus, P. W. (1983) Arachidonate metabolism in vascular disorders. *J. Clin. Invest. 72*, 1521–1525.
3. Vane, J., and Corin, R. E. (2003) Prostacyclin: A vascular mediator. *Eur. J. Vasc. Endovasc. Surg. 26*, 571–578.
4. Narumiya, S., Sugimoto, Y., and Ushikubi, F. (1999) Prostanoid receptors: Structures, properties, and functions. *Physiol. Rev. 79*, 1193–1226.
5. Wise, H. (2003) Multiple signaling options for prostacyclin. *Acta Pharmacol. Sin. 24*, 625–630.
6. Braissant, O., Foufelle, F., Scotto, C., Dauca, M., and Wahli, W. (1996) Differential expression of peroxisome proliferator-activated receptors (PPARs): Tissue distribution of PPAR-α, -β, and -γ in the adult rat. *Endocrinology 137*, 354–366.
7. Kliewer, S. A., Forman, B. M., Blumberg, B., Ong, E. S., Borgmeyer, U., Mangelsdorf, D. J., Umesono, K., and Evans, R. M. (1994) Differential expression and activation of a family of murine peroxisome proliferator-activated receptors. *Proc. Natl. Acad. Sci. U.S.A. 91*, 7355–7359.
8. Becker, J., Delayre-Orthez, C., Frossard, N., and Pons, F. (2006) Regulation of inflammation by PPARs: A future approach to treat lung inflammatory diseases? *Fundam. Clin. Pharmacol. 20*, 429–447.
9. Lefebvre, P., Chinetti, G., Fruchart, J. C., and Staels, B. (2006) Sorting out the roles of PPARα in energy metabolism and vascular homeostasis. *J. Clin. Invest. 116*, 571–580.
10. Fajas, L., Auboeuf, D., Raspé, E., Schoonjans, K., Lefebvre, A. M., Saladin, R., Najib, J., Laville, M., Fruchart, J. C., Deeb, S., Vidal-Puig, A., Flier, J., Briggs, M. R., Staels, B., Vidal, H., and Auwerx, J. (1997) The organization, promoter analysis, and expression of the human PPARγ gene. *J. Biol. Chem. 272*, 18779–18789.
11. Falcettia, E., Flavell, D. M., Staels, B., Tinker, A., Haworth, S. G., and Clapp, L. H. (2007) IP receptor-dependent activation of PPARγ by stable prostacyclin analogues. *Biochem. Biophys. Res. Commun. 360*, 821–827.
12. Hodnett, B. L., Dearman, J. A., Carter, C. B., and Hester, R. L. (2009) Attenuated PGI_2 synthesis in obese Zucker rats. *Am. J. Physiol. 296*, R715–R721.
13. Massiera, F., Saint-Marc, P., Seydoux, J., Murata, T., Kobayashi, T., Narumiya, S., Guesnet, P., Amri, E. Z., Negrel, R., and Ailhaud, G. (2003) Arachidonic acid and prostacyclin signaling promote adipose tissue development: A human health concern? *J. Lipid Res. 44*, 271–279.
14. Páramo, J. A., Orbe, J., Beloqui, O., Colina, I., Benito, A., Rodríguez, J. A., and Díez, J. (2008) Association of age, inflammatory markers and subclinical atherosclerosis in subjects free from cardiovascular disease. *Med. Clin. (Barcelona) 131*, 361–366.
15. Stary, H. C. (2003) Atlas of Atherosclerosis: Progression and Regression, 2nd ed., Parthenon Publishing Group, New York.
16. Strong, J. P., Malcom, G. T., McMahan, C. A., Tracy, R. E., Newman, W. P., III, and Herderick, E. E. (1999) Prevalence and extent of atherosclerosis in adolescents and young adults: Implications for prevention from the Pathobiological Determinants of Atherosclerosis in Youth Study. *JAMA, J. Am. Med. Assoc. 281*, 727–735.
17. Ruan, K. H., Deng, H., and So, S. P. (2006) Engineering of a protein with cyclooxygenase and prostacyclin synthase activities that converts arachidonic acid to prostacyclin. *Biochemistry 45*, 14003–14011.
18. Ruan, K. H., So, S. P., Cervantes, V., Wu, H., Wijaya, C., and Jentzen, R. R. (2008) An active triple-catalytic hybrid enzyme engineered by linking cyclo-oxygenase isoform-1 to prostacyclin synthase that can constantly biosynthesize prostacyclin, the vascular protector. *FEBS J. 275*, 5820–5829.
19. Ruan, K. H., So, S. P., Wu, H., and Cervantes, V. (2008) Large-scale expression, purification, and characterization of an engineered prostacyclin-synthesizing enzyme with therapeutic potential. *Arch. Biochem. Biophys. 480*, 41–50.
20. Farh, K. K., Grimson, A., Jan, C., Lewis, B. P., Johnston, W. K., Lim, L. P., Burge, C. B., and Bartel, D. P. (2005) The widespread impact of mammalian microRNAs on mRNA repression and evolution. *Science 310*, 1817–1821.
21. Pasquinelli, A. E., Hunter, S., and Bracht, J. (2005) MicroRNAs: A developing story. *Curr. Opin. Genet. Dev. 15*, 200–205.
22. Ambros, V. (2004) The functions of animal microRNAs. *Nature 431*, 350–355.
23. Du, T., and Zamore, P. D. (2007) Beginning to understand microRNA function. *Cell Res. 17*, 661–663.
24. Hwang, H. W., and Mendell, J. T. (2006) MicroRNAs in cell proliferation, cell death, and tumorigenesis. *Br. J. Cancer 94*, 776–780.
25. Jovanovic, M., and Hengartner, M. O. (2006) miRNAs and apoptosis: RNAs to die for. *Oncogene 25*, 6176–6187.
26. Rane, S., Sayed, D., and Abdellatif, M. (2007) MicroRNA with a MacroFunction. *Cell Cycle 6*, 1850–1855.
27. Van Rooij, E., and Olson, E. N. (2007) MicroRNAs: Powerful new regulators of heart disease and provocative therapeutic targets. *J. Clin. Invest. 117*, 2369–2376.
28. Blenkiron, C., and Miska, E. A. (2007) miRNAs in cancer: Approaches, aetiology, diagnostics and therapy. *Hum. Mol. Genet. 16*, R106–R113.
29. Poy, M. N., Eliasson, L., Krutzfeldt, J., Kuwajima, S., Ma, X., Macdonald, P. E., Pfeffer, S., Tuschl, T., Rajewsky, N., Rorsman, P., and Stoffel, M. (2004) A pancreatic islet-specific microRNA regulates insulin secretion. *Nature 432*, 226–230.
30. Esau, C., Davis, S., Murray, S. F., Yu, X. X., Pandey, S. K., Pear, M., Watts, L., Booten, S. L., Graham, M., McKay, R., Subramaniam, A., Propp, S., Lollo, B. A., Freier, S., Bennett, C. F., Bhanot, S., and Monia, B. P. (2006) miR-122 regulation of lipid metabolism revealed by in vivo antisense targeting. *Cell Metab. 3*, 87–98.
31. Rodriguez, A., Vigorito, E., Clare, S., Warren, M. V., Couttet, P., Soond, D. R., van Dongen, S., Grocock, R. J., Das, P. P., Miska, E. A., Vetrie, D., Okkenhaug, K., Enright, A. J., Dougan, G., Turner, M., and Bradley, A. (2007) Requirement of bic/microRNA-155 for normal immune function. *Science 316*, 608–611.
32. Kajimoto, K., Naraba, H., and Iwai, N. (2006) MicroRNA and 3T3-L1 pre-adipocyte differentiation. *RNA 12*, 1626–1632.
33. Tang, Q. Q., Zhang, J. W., and Daniel Lane, M. (2004) Sequential gene promoter interactions by C/EBPβ, C/EBPα, and PPARγ during adipogenesis. *Biochem. Biophys. Res. Commun. 318*, 213–218.

34. Yun, S. J., Kim, E. K., Tucker, D. F., Kim, C. D., Birnbaum, M. J., and Bae, S. S. (2008) Isoform-specific regulation of adipocyte differentiation by Akt/protein kinase Bα. *Biochem. Biophys. Res. Commun. 371*, 138–143.
35. Nakae, J., Kitamura, T., Kitamura, Y., Biggs, W. H., III, Arden, K. C., and Accili, D. (2003) The forkhead transcription factor Foxo1 regulates adipocyte differentiation. *Dev. Cell 4*, 119–129.
36. Fritzius, T., and Moelling, K. (2008) Akt- and Foxo1-interacting WD-repeat-FYVE protein promotes adipogenesis. *EMBO J. 27*, 1399–1410.
37. Kasza, Z., Fetalvero, K. M., Ding, M., Wagner, R. J., Acs, K., Guzman, A. K., Douville, K. L., Powell, R. J., Hwa, J., and Martin, K. A. (2009) Novel signaling pathways promote a paracrine wave of prostacyclin-induced vascular smooth muscle differentiation. *J. Mol. Cell. Cardiol. 46*, 682–694.